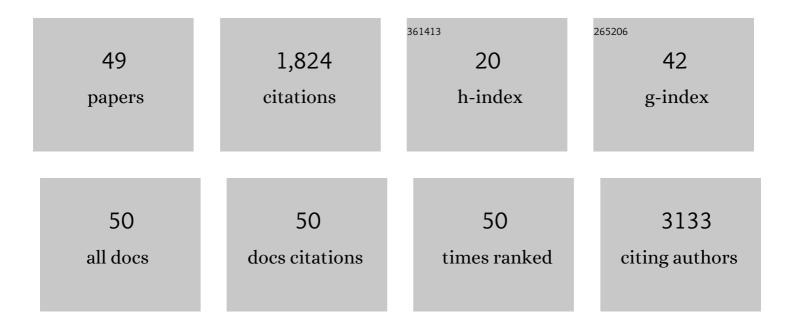
Fei Long

List of Publications by Year in descending order

Source: https://exaly.com/author-pdf/8892475/publications.pdf Version: 2024-02-01



FELLONG

#	Article	IF	CITATIONS
1	Accelerated Crystal Growth in >16% Printed MA _{<i>x</i>} FA _{<i>y</i>} Cs _{<i>z</i>} PbI ₃ Perovskite Solar Cells from Aqueous Inks. ACS Sustainable Chemistry and Engineering, 2022, 10, 5225-5232.	6.7	1
2	Rich 1Tâ€MoS ₂ Nanoflowers Decorated on Reduced Graphene Oxide Nanosheet for Ultraâ€Quick Zn ²⁺ Storage. Batteries and Supercaps, 2022, 5, .	4.7	4
3	Stable organic-inorganic hybrid bismuth-halide: Exploration of crystal-structural, morphological, thermal, spectroscopic and optoelectronic properties. Journal of Molecular Structure, 2022, 1264, 133102.	3.6	8
4	Modifying SnO ₂ with Polyacrylamide to Enhance the Performance of Perovskite Solar Cells. ACS Applied Materials & Interfaces, 2022, 14, 34143-34150.	8.0	27
5	Role of seed layer in van der Waals growth of vanadium dioxide film on mica prepared by chemical solution deposition. Journal of Sol-Gel Science and Technology, 2021, 98, 24-30.	2.4	4
6	Synthesis, Crystal Structure, Optical Properties and Stability of New Bismuthâ€Based Organicâ€Inorganic Compounds (C ₆ H ₉ N ₂) _a Bi _b X _c (X=Cl, Br, I). ChemistrySelect, 2021, 6, 1099-1106.	1.5	6
7	Unique three-dimensional hierarchical heterogeneous MoS2/graphene structures as a high-performance anode material for lithium-ion batteries. Ionics, 2021, 27, 1977-1986.	2.4	5
8	Fabrication and mechanical properties of boron nitride nanotube reinforced boron carbide ceramics. Journal of the Ceramic Society of Japan, 2021, 129, 187-194.	1.1	4
9	Synthesis, Structure, and Photoelectric Properties of a Novel 0-Dimensional Organic–Inorganic Hybrid Perovskite (2-5-py) ₂ MnBr ₄ . Journal of Physical Chemistry C, 2021, 125, 22898-22906.	3.1	13
10	Synthesis, crystal structure, photoluminescence properties of organic-inorganic hybrid materials based on ethylenediamine bromide. Journal of Saudi Chemical Society, 2020, 24, 52-60.	5.2	21
11	Hollow MXene Sphere/Reduced Graphene Aerogel Composites for Piezoresistive Sensor with Ultraâ€High Sensitivity. Advanced Electronic Materials, 2020, 6, 1901064.	5.1	137
12	One-Pot Hydrothermal Synthesis of La-Doped ZnIn2S4 Microspheres with Improved Visible-Light Photocatalytic Performance. Nanomaterials, 2020, 10, 2026.	4.1	23
13	Rare Earth Ion Yb3+ Doping of Bi2WO6 with Excellent Visible-light Photocatalytic Activity. Journal Wuhan University of Technology, Materials Science Edition, 2020, 35, 348-355.	1.0	12
14	Facile synthesis of few-layer MoS ₂ in MgAl-LDH layers for enhanced visible-light photocatalytic activity. RSC Advances, 2019, 9, 24280-24290.	3.6	23
15	Graphene Aerogel Broken to Fragments for a Piezoresistive Pressure Sensor with a Higher Sensitivity. ACS Applied Materials & Interfaces, 2019, 11, 33165-33172.	8.0	58
16	Space-Confined Effect One-Pot Synthesis of γ-AlO(OH)/MgAl-LDH Heterostructures with Excellent Adsorption Performance. Nanoscale Research Letters, 2019, 14, 281.	5.7	32
17	Crystal structure and electrical conduction of the organic–inorganic compound (C6H9N2)2ZnI4. Polyhedron, 2019, 164, 48-54.	2.2	5
18	Noble metal-free NiS2 with rich active sites loaded g-C3N4 for highly efficient photocatalytic H2 evolution under visible light irradiation. Journal of Colloid and Interface Science, 2019, 534, 343-349.	9.4	57

Fei Long

#	Article	IF	CITATIONS
19	Oneâ€Dimensional ABX ₃ â€Type Fluorescent Crystal: CH ₃ NH ₃ ZnI ₃ . Crystal Research and Technology, 2018, 53, 1800017.	1.3	5
20	Synthesis of novel and stable g-C ₃ N ₄ -Bi ₂ WO ₆ hybrid nanocomposites and their enhanced photocatalytic activity under visible light irradiation. Royal Society Open Science, 2018, 5, 171419.	2.4	27
21	Crystal structure, optical behavior and electrical conduction of the new organic–inorganic compound CH3NH3CdI3. Journal of Materials Science: Materials in Electronics, 2018, 29, 9821-9828.	2.2	7
22	Crystal structure and electrical conduction of the new organic-inorganic compound (CH 2) 2 (NH 3) 2 Cdl 4. Journal of Molecular Structure, 2018, 1156, 450-456.	3.6	6
23	Effective Preparation of Oneâ€Dimensional Boronâ€Nitride―Nanotubeâ€Supported Nanosheet Hierarchical Structures and Their Optical/Adsorption Properties. ChemistrySelect, 2018, 3, 10832-10836.	1.5	3
24	Synthesis of M (M=Co2+, Co2+/Ni2+)-doped FeS2 Nanospheres with Enhanced Visible-light-induced Photocatalytic Activity. Journal Wuhan University of Technology, Materials Science Edition, 2018, 33, 802-811.	1.0	7
25	A Facile Approach for the Synthesis of Zn2SnO4/BiOBr Hybrid Nanocomposites with Improved Visible-Light Photocatalytic Performance. Nanomaterials, 2018, 8, 313.	4.1	25
26	Synthesis of Highâ€Quality Wurtzite Cu ₂ ZnSn(S _{1<i>â^'x</i>} ,Se _{<i>x</i>}) ₄ Nanocrystals With Nonâ€Toxic Selenium Precursor and the Photoelectrochemical Performance of ZnO NAs/CZTSSe Heterojunction. Solar Rrl, 2018, 2, 1800015.	5.8	15
27	Highly Stretchable and Self-Healable Supercapacitor with Reduced Graphene Oxide Based Fiber Springs. ACS Nano, 2017, 11, 2066-2074.	14.6	413
28	Superelastic and ultralight electron source from modifying 3D reduced graphene aerogel microstructure. Nano Energy, 2017, 33, 280-287.	16.0	26
29	Understanding the growth mechanism of wurtzite Cu 2 ZnSnS 4 nanocrystals and the photodegradation properties. Materials and Design, 2017, 123, 24-31.	7.0	13
30	A high performance wire-shaped flexible lithium-ion battery based on silicon nanoparticles within polypyrrole/twisted carbon fibers. RSC Advances, 2017, 7, 26601-26607.	3.6	23
31	Glass fabrics self-cracking catalytic growth of boron nitride nanotubes. Solid State Sciences, 2017, 64, 23-28.	3.2	8
32	Mass Production of Bi3NbO7 / Bi2Zn2/3Nb4/3O7 composites and their visible-light photocatalytic activity. Journal Wuhan University of Technology, Materials Science Edition, 2017, 32, 403-407.	1.0	0
33	Ribbon-like Cu doped V6O13 as cathode material for high-performance lithium ion batteries. Journal Wuhan University of Technology, Materials Science Edition, 2017, 32, 1397-1401.	1.0	7
34	Ultrathin g-C3N4 Nanosheet-Modified BiOCl Hierarchical Flower-Like Plate Heterostructure with Enhanced Photostability and Photocatalytic Performance. Crystals, 2017, 7, 266.	2.2	34
35	In situ controlled rapid growth of novel high activity TiB ₂ /(TiB ₂ –TiN) hierarchical/heterostructured nanocomposites. Beilstein Journal of Nanotechnology, 2017, 8, 2116-2125.	2.8	4
36	Facile Synthesis, Characterization, and Visible-light Photocatalytic Activities of 3D Hierarchical Bi2S3 Architectures Assembled by Nanoplatelets. Crystals, 2016, 6, 140.	2.2	11

Fei Long

#	Article	IF	CITATIONS
37	Synthesis, characterization and enhanced visible-light photocatalytic activity of Zn2SnO4/C nanocomposites with truncated octahedron morphology. Ceramics International, 2016, 42, 13893-13899.	4.8	28
38	Solid state synthesis of nonstoichiometric Bi2WO6/Bi2O3 composites as visible-light photocatalyst. Ionics, 2016, 22, 2347-2353.	2.4	9
39	Synthesis, characterization and thermal stability of CeO2 stabilized ZrO2 ultra fine nanoparticles via a sol-gel route. Journal Wuhan University of Technology, Materials Science Edition, 2016, 31, 1245-1249.	1.0	2
40	Piezoresistive Sensor with High Elasticity Based on 3D Hybrid Network of Sponge@CNTs@Ag NPs. ACS Applied Materials & Interfaces, 2016, 8, 22374-22381.	8.0	176
41	A Flexible Integrated System Containing a Microsupercapacitor, a Photodetector, and a Wireless Charging Coil. ACS Nano, 2016, 10, 11249-11257.	14.6	166
42	Solvent-free catalytic synthesis and optical properties of super-hard phase ultrafine carbon nitride nanowires with abundant surface active sites. RSC Advances, 2016, 6, 23272-23278.	3.6	22
43	Preparation of nano-sized zirconium carbide powders through a novel active dilution self-propagating high temperature synthesis method. Journal Wuhan University of Technology, Materials Science Edition, 2015, 30, 729-734.	1.0	8
44	Microwave-hydrothermal synthesis of Co-doped FeS2 as a visible-light photocatalyst. Journal of Materials Science, 2015, 50, 1848-1854.	3.7	36
45	Compared selection of pretreatment technology for cassava starch wastewater treated by anaerobic process. , 2011, , .		1
46	Discussion of the maximum design current velocity of small towns' drainage pipelines in South China. , 2011, , .		0
47	Synthesis and Characterization of Arsenate/Phosphate Fluorapatite Solid Solutions. Metallurgical and Materials Transactions A: Physical Metallurgy and Materials Science, 2009, 40, 2659-2663.	2.2	7
48	Fabrication, characterization and photocatalytic activity of La-doped ZnO nanowires. Journal of Alloys and Compounds, 2009, 484, 410-415.	5.5	183
49	Synthesis, Characterization, and Photocatalytic Activity of Zn-Doped SnO ₂ Hierarchical Architectures Assembled by Nanocones. Journal of Physical Chemistry C, 2009, 113, 9071-9077.	3.1	111